Neural network with k-fold cross validation for oil palm fruit ripeness prediction

Minarni Shiddiq[1], Feri Candra[2], Barri Anand[2], Mohammad Fisal Rabin[1]
[1]Department of Physics, Faculty of Mathematics and Natural Sciences, University of Riau, Pekanbaru, Indonesia
[2]Department of Electrical Engineering, Faculty of Engineering, University of Riau, Pekanbaru, Indonesia

Article Info

ABSTRACT

The combination of hyperspectral imaging and artificial neural network (ANN) can predict fruit ripeness. This work investigated the application of hyperspectral imaging and ANN models with the k-fold cross-validation method for ripeness prediction of oil palm fresh fruit bunches (FFB) for in-line sorting and grading machine vision. Crude palm oil (CPO) is an exporting commodity for countries such as Indonesia and Malaysia. Oil palm FFB ripeness determines the quality of CPO. The unique shapes and colors of FFBs need innovative methods to substitute tedious and cumbersome manual sorting and grading. The oil palm FFB samples used in this study were categorized previously based on color and loosed fruits. We applied the Savitzky-Golay (SG) smoothing filter and 7-fold cross-validation for hyperspectral datasets before being used for the ANN models and a confusion matrix to find the ANN model accuracies. We obtained 72 data points after SG filter and data selection from 523 data points. The prediction results showed an average accuracy of 79.48%, in which three folds with k of 2, 5, and 7 gave the highest accuracy of 90%. The results confirmed the potential use of hyperspectral imaging, with k-fold cross-validation and ANN models for ripeness prediction of oil palm FFBs.

Corresponding Author:

Minarni Shiddiq
Department of Physics, Faculty of Mathematics and Natural Sciences, University of Riau
Kampus Bina Widya, Jl. HR. Soebrantas Km. 12.5 Simpang Baru, Pekanbaru 28293, Riau, Indonesia
Email: minarni.shiddiq@lecturer.unri.ac.id

1. INTRODUCTION

Computer vision is an imaging technique using a computer and a camera that has had many applications in agriculture. It has flourished in the last two decades for evaluating the quality of fruits and vegetables. Ripeness, external or internal damages, and chemical contents are among the quality attributes often used for classifications and predictions of fruits and vegetables [1]. Machine vision uses computer vision with other instruments to perform automatic tasks, especially for non-destructive and fast sorting and grading of fruits and vegetables. Machine vision aims to substitute tedious, time-consuming sorting and grading process [2]. Computer vision obtains images of fruits and vegetables and performs many steps, such as preprocessing, segmentation, feature extraction, and classification. Information extracted from the resulting images can represent the qualities of fruits and vegetables based on external and internal characteristics [3].

Computer vision methods have evolved rapidly due to technological advances in computers, image detectors, and image processing methods. Conventional computer vision uses a color camera and white light. It is applied to assess the external characteristics of fruits, such as color, shapes, sizes, or textures. Spectral imaging is a computer vision technique that combines imaging methods and spectroscopy. It has not only

spatial but also spectral information. Spectral imaging includes hyperspectral and multispectral imaging. Hyperspectral imaging has more advantages over traditional imaging due to continuous wavelength region coverage, providing higher image resolution [4]. It can predict maturity and ripeness based on the internal characteristics of fruits and vegetables [5]. Hyperspectral imaging has been used widely in food industries for evaluating the quality and safety of food products [6]. It has been able to predict apple internal quality [7], moisture content (MC), dry matter content (DMC), firmness (F) of dates [8], and dry matter content of avocado [9].

Many types of computer vision require machine learning to classify fruits and predict fruit qualities, including hyperspectral imaging. Machine learning is part of artificial intelligence used intensively in computer vision. It contains algorithms to analyze, learn, and make decisions from datasets. Deep learning is the advancement of machine learning which is more robust because it has complex algorithms. It is in demand since many multifaceted problems are found in fruit and vegetable classification [10]. Artificial neural networks (ANN) and convolutional neural networks (CNN) are two types of deep learning methods used in many applications in fruit classification. This machine learning type has been applied with hyperspectral imaging to classify or predict fruit physical-chemical characteristics, such as predicting firmness and soluble solid contents of Korla pear [11] and tomatos [12].

Classification of fruit and vegetables using hyperspectral imaging and ANN model need reliable input datasets. Some image preprocessing steps are essential for hyperspectral datasets due to random noise from many sources, such as misalignments of optical components, sensor sensitivity, and inappropriate reflectance calibrations [13]. One of the preprocessing techniques for hyperspectral datasets is Savitzky-Golay (SG) filtering. SG filtering performs curve fitting successive subsets of an adjacent dataset using the least-squares digital polynomial smoothing filter [14]. This method has been used for hyperspectral images of peanut seed vigor [15] and strawberry water content estimation and ripeness classification [16]. The next step after SG filtering is to validate the training datasets using k-fold cross-validation. K-fold cross-validation is one of the methods used to validate an estimation model and find reliable variables [17]. It is a popular procedure for evaluating the performance of classification algorithms [18]. This technique is part of preprocessing methods used in machine learning for wide-ranging problems, such as predicting the notch frequency of an ultra-wideband (UWB) antenna [19] and quality attributes of orange fruit using hyperspectral imaging [20].

Crude palm oil (CPO) is one of the export commodities which contribute to the economic growth of countries in Southeast Asia, such as Indonesia and Malaysia. However, these industries have faced crucial problems such as CPO quality, process automation, and environmental issues that challenge the industry sustainability. Small holder plantations have less access to certification bodies [21]. Oil palm fresh fruit bunches (FFBs) are the source of CPO. The main CPO quality attributes are oil contents and free fatty acids, which relate to the ripeness of oil palm FFBs. High oil contents and low free fatty acids are the desirable qualities of oil palm FFBs arriving in a palm oil refinery. Sorting and grading FBBs are very crucial processes in obtaining high-quality FFBs. However, in practice, they are still done manually and destructively. Electronic sensors and imaging techniques were capable to predict the ripeness levels of oil palm FFBs and improve the sorting and grading processes. A detection system has used a 670 nm light source and an optical sensor to determine the FFB ripeness levels [22]. Moreover, imaging techniques such as thermal imaging [23], laser-induced fluorescence imaging [24], and near-infrared (NIR) spectroscopy [25] have been proposed to determine and predict FFB ripeness.

In this study, we developed a hyperspectral imaging-based machine vision that suits the environment in the reception area at a palm oil refinery facility. The system consisted of a conveyor unit, a hyperspectral imaging unit, a light-tight box, and an image processing software unit. Hyperspectral imaging has been used for oil palm FFB ripeness detection with K-mean clustering analysis [26] and ANN model [27]. Most of the innovations regarding the prediction of oil palm applied traditional computer vision and other instruments. Traditional computer vision uses a webcam or smartphone with color spaces such as red green blue (RGB) or hue saturated value (HSV). Bulge and commercial spectrometers were also used which are difficult to integrate for real-time machine vision. Some systems were on a laboratory scale. More study is necessary to implement efficiently hyperspectral imaging and ANN model in a real-time oil palm FFB sorting and grading machine vision. We proposed a feed-forward ANN model to predict FFB ripeness levels, categorized as unripe (immature) and ripe (mature). We used SG filtering and k-fold cross-validation techniques on the datasets of spectral reflectance intensities, resulting from the hyperspectral imaging system before being used in the ANN model. A confusion matrix measured the accuracy of the prediction. We used self-written Matlab-based software to do the image processing and analysis process. This paper contains an introduction, method, results, and discussion, followed by a conclusion.

2. METHOD

Designing ANN models with k-fold cross-validation for predicting the ripeness levels of oil palm FFBs required some stages. The first stage was the acquisition of FFB images using a hyperspectral imaging system. The second was to resize and reduce the format of the hyperspectral images and calibrate each image using a white reference image and a dark image. The next stage was to impose the region of interest (ROI) and average to obtain spectral data represented by the average reflectance intensities versus wavelength for each FFB. Later, SG smoothing and K-fold cross-validation would validate the spectral datasets for the ANN model. The last step was to design and implement the ANN on the hyperspectral datasets. We used a confusion matrix to measure the prediction performance and a graphical user interface (GUI) to display the SG smoothing and ANN prediction.

2.1. Hyperspectral images

The hyperspectral images of oil palm FFB were acquired using a hyperspectral imaging system, as shown in Figure 1 [26]. The system consisted of a Sentech NIR Monochrome camera with a resolution and sensor size of 2.2 MP and 2/3", a specim impector V10 spectrograph in 400-1000 nm (Vis-NIR) region, a pair of Dolan Jenner halogen line light sources, a belt conveyor, and a control unit. The camera has Senko 25 mm, 2/3" lens. The hyperspectral imaging system used a line-scanning scheme controlled using a MATLAB-based acquisition program and contained in a light-tight or black box to minimize room light. The distance from the camera lens end to the conveyor surface was 83 cm. The line lights were positioned at each box side forming 45° angle to the vertical line.
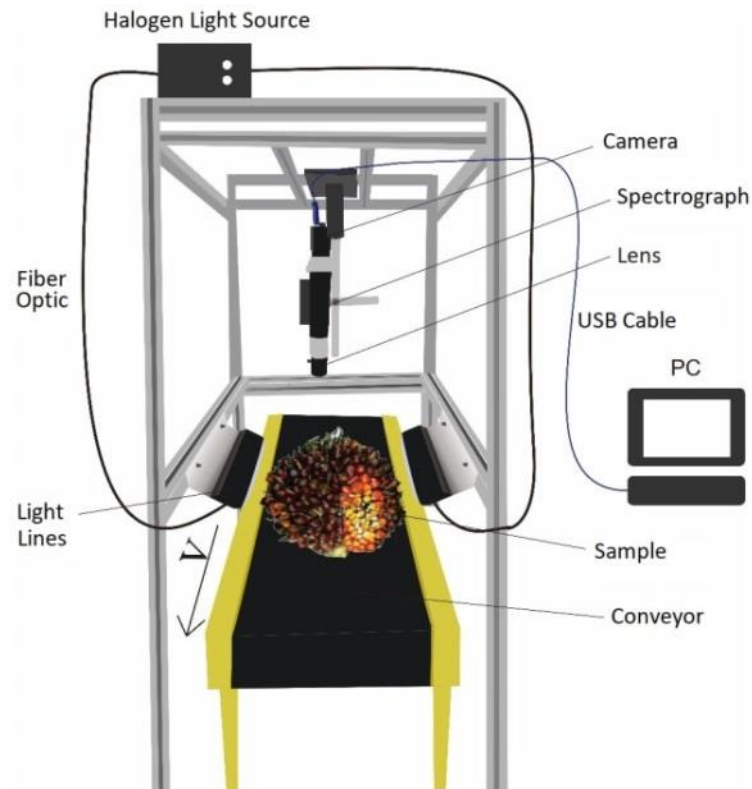

Figure 1. The optical and hardware components of the hyperspectral system

This study used samples of oil palm FFBs from a vicinity plantation about 7 kilometers from our laboratory. The harvested Tenera FFB samples were categorized previously as fractions F0, F1, F2, F3, and F4 based on color changes and the number of loosed fruits [23], helped by experienced harvesters. The standards for ripeness fractions categorize F0 and F1 as unripe, F2 and F3 as ripe, and F4 as the overripe. The FFB fractions were classified further for this study as unripe or immature (F0, F1) and ripe or mature (F2, F3, and F4) since F4 fraction FFBs are acceptable in the sorting area. Table 1 shows the color images of unripe and ripe oil palm FFBs captured from three sides, where the FFB back side image was uncounted due to

infertile fruits on half of the side. Unripe or immature FFBs have colors ranging from blackish to purple, while the ripe or mature FFBs have red to orange colors with some loosed fruit from bunches. Each FFB has a ripeness fraction symbol on its stalk for easy identification.

Image acquisition was performed on each oil palm FFB moving on a conveyor. First, a calibration was made for the hyperspectral optical unit using three visible lasers with 405 nm, 532 nm, and 650 nm wavelengths. It aimed to calibrate pixels on the wavelength axis of a hyperspectral cube image where the Specim v10 spectrograph specim has a wavelength range of 400-1,000 nm. We have 23 image acquisition times for building the ANN model dataset. Each had 8 FFBs consisting of 4 ripeness fractions (184 FFBs). The FFBs were scanned immediately within 24 hours after harvesting to maintain the ripeness levels. The image acquisition used a line scan scheme with 250 frames per second speed. We also took white and dark reference images. The acquisition process saved the recorded images in matfile (.mat) format for image processing.

Table 1. Images of three sides of an oil palm bunch

Ripeness category	Front side	Right side	Left side
Unripe (immature)			
Ripe (mature)			

2.2. Image preprocessing and spectral mean conversion

The image processing for oil palm FFB images aimed to obtain the reflectance intensities of light in the wavelength range of 400–1000 nm. The oil palm FFB images obtained using the hyperspectral system and MATLAB acquisition software have a size of 1088×2048 px in 4D format. The first step of the image processing was to resize the images for faster image processing time and convert into 3D format and store them in Matfile (mat) format. The 3D spectral images had a matrix format of (λ, y, x) with λ as wavelength and x, y as spatial coordinates. One of the essential steps in spectral image processing is to correct each spectral image using a standard white reference image and a dark image. The (1) shows the relation of the corrected intensity (I_c) as the function of I_r, I_d, and I_w were the raw hyperspectral image intensity, the dark image intensity, and the white reference image intensity, respectively [26].

$$I_c = \frac{I_r - I_d}{I_w - I_d}$$

(1)

The resized, reduced, and corrected spectral images had a dimension of (λ, y, x). Then, the spectral images were converted to images of a matrix format of (x, y, λ). The final hyperspectral images had a size of (1024×1088×544), which has 544 wavelengths. Spectral mean conversion for each image was performed to get mean reflectance intensities for a wavelength range of 400–1,000 nm for each FFB sample [13]. The image processing stage obtained 523 useable spectral data points.

2.3. Smoothing and k-fold cross-validation

Smoothing is a preprocessing step before the hyperspectral images available for the ANN classifier. The hyperspectral images contain random noise due to optical misalignment, inhomogeneous lighting, and sensor noise. Here SG filter functioned to smooth the dataset. After conversation and resizing, the spectral data

become a matrix with a size of $N \times 544$, which N is the number of spectral data. It means each spectral data has a spectrum with wavelengths of 544. Each spectrum plot consists of reflectance intensity on the y-axis and wavelength on the x-axis. In this study, we used the MATLAB program to do SG smoothing. SG filter was performed on a window portion of the hyperspectral spectrum using a polynomial function to fit by the least square method [14]. We used framelen of 11 and an order of 3 for the polynomials, with a dt of 1/551.

The training and testing data need to be compatible with the ANN classifier. Therefore, data selection is crucial. The total number of data points obtained previously was 523. However, not all the data points are suitable for designing the ANN model. Data selection tries to find the average of the data points and choose the data point closest value to the average value. This technique aims to reduce error when applied to the ANN classifier. This process resulted in 72 data points, ready to be inputted into the ANN classifier.

Cross-validation is one of the machine learning techniques used to evaluate and test a classifier model. The cross-validation method has many forms, which include k-fold cross validation. The k-fold cross-validation aims to select training and testing datasets to have ANN models with higher accuracy. Another objective of k-fold cross validation is to avoid a classifier mode having an overfitting condition.

We divided evenly, randomly the 72 data points into seven parts or subsets [18] as shown in Table 2. Each subset is called the k-fold. There existed 7-fold (fold 1–fold 7) where folds 3 and 4 had 11 data points, and other folds had 10 data points, respectively. Iteration of fold 3 and fold 4 had 11 testing data points and 61 training data points hence training ratio was 15:85. For folds 1, 2, 5, 6, and 7, each had 10 testing data points and 62 training data points, hence had a training ratio of 13:87. Each fold was tested for its accuracy and compared to the other folds. Fold with the highest accuracy will be used for the ANN model.

Table 2 shows the partition of the 1st to 7th fold with seven iterations. At the first iteration, 1st fold subset was used as testing data, while 2nd to 7th fold subsets were the training data. Similarly, at the second iteration, the 2nd fold subset was used as the testing data, 1st fold, and the 3rd fold-the 7th fold subsets were the training data. The iteration process would continue correspondingly. After the iteration process, the accuracy of each subset was calculated. This process intended to find the average accuracy level of the designed ANN model and which k-fold had the highest accuracy.

Table 2. Separation of training and testing data

Cross validation	Fold 1	Fold 2	Fold 3	Fold 4	Fold 5	Fold 6	Fold 7
Iteration 1	Test	Train	Train	Train	Train	Train	Train
Iteration 2	Train	Test	Train	Train	Train	Train	Train
Iteration 3	Train	Train	Test	Train	Train	Train	Train
Iteration 4	Train	Train	Train	Test	Train	Train	Train
Iteration 5	Train	Train	Train	Train	Test	Train	Train
Iteration 6	Train	Train	Train	Train	Train	Test	Train
Iteration 7	Train	Train	Train	Train	Train	Train	Test

2.4. Designing and implementation of ANN model

After completing the k-fold cross-validation process, we designed an ANN. The ANN was a feedforward ANN with backpropagation functions. Figure 2 shows the architecture of the ANN. It has 499-10-1 that indicates 499 inputs, 10 hidden layers, and one 1 output. Input data consisted of 72 data points, each having a value of 544. The ANN used training ratios of 13:87 and 15:85 as described previously in k-fold cross-validation process.

The next step was to use the ANN model for the oil palm FFB ripeness prediction. Before predicting the ripeness levels of oil palm FFB, the ANN was trained using data subsets from the k-fold cross-validation until reaching the optimal results. The ANN parameters include epochs of 100 and learning rate of 0.1. The ANN system was written in MATLAB language of version 9.8.0.1323502 and equipped with GUI. GUI displayed the hyperspectral spectrum before and after smoothing using the SG filter. It can also show the estimation result for ripeness levels of oil palm FFBs. The ANN model was implemented on the hyperspectral images taken using the imaging system. The ANN algorithms were considered potential to be implemented if the prediction accuracy was more than 75%.

2.5. Accuracy analysis using confusion matrix

Using metrics is the final step to measure the accuracy of the ANN model for the hyperspectral images. Confusion matrix is one of the popular methods to measure ANN classifier performance. A confusion matrix aims to describe estimation model performance in a chart shown in Figure 3 [28]. The chart in Figure 3 contains the accuracy and statistical parameters, such as error rate, recall, and precision. In this study, the confusion matrix was used to describe the performance of each fold validation.
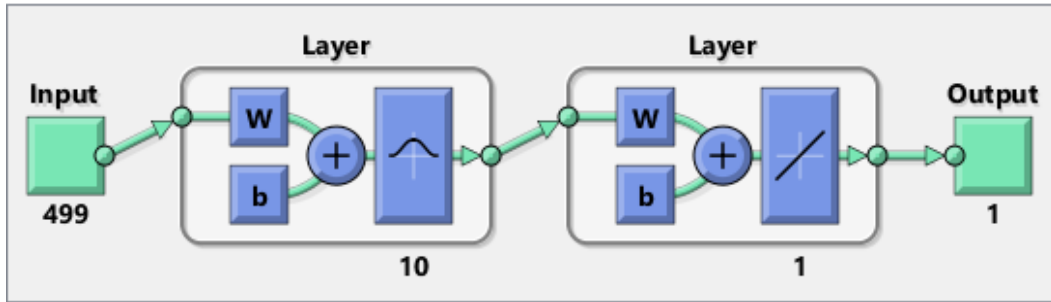
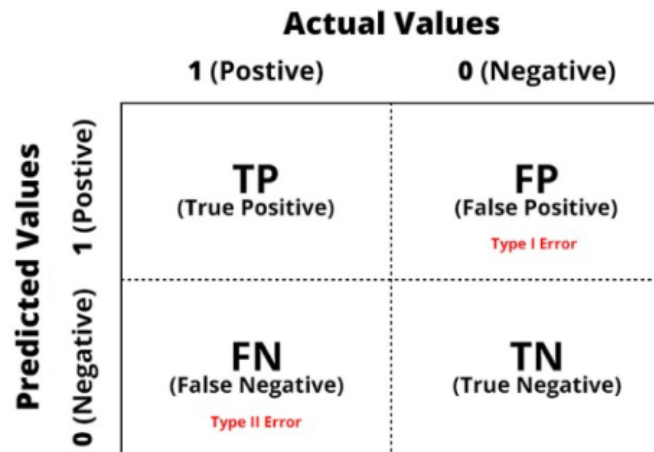Figure 2. Structure of the designed neural network

Figure 3. Confusion matrix of prediction and actual values

The accuracy calculation uses positive and negative values, which are 1 for positive and 0 for negative. However, for this prediction, the result of the negative value means unripe FFB, while the positive value means ripe FFB. Equations for accuracy prediction, error rate, recall, and precision [29] are described in (2)-(5), respectively. Here, true positive (TP), true negative (TN), false positive (FP), and false negative (FN) are defined as TP=correct prediction result with positive value, TN=correct prediction result with negative value, FP=incorrect prediction result with positive value, and FN=incorrect prediction result with negative value.

$$Accuracy = \frac{TP+TN}{TP+TN+FP+FN} \times 100\% \tag{2}$$

$$Error\ Rate = \frac{FP+FN}{TP+TN+FP+FN} *\times 100\% \tag{3}$$

$$Recall = \frac{TP}{TP+TN} \times 100\% \tag{4}$$

$$Precision = \frac{TP}{TP+FP} \times 100\% \tag{5}$$

3. RESULTS AND DISCUSSION
3.1. Savitzky-Golay smoothing

Figure 4 shows the original hyperspectral spectral of an oil palm fresh fruit bunch compared to the filtered spectrum using the SG algorithm. SG filter is one of the preprocessing techniques, which is also applied to hyperspectral images [30]. Hyperspectral spectra have noises due to the complexity of the hyperspectral imaging system with many electronic and optical components involved. Therefore, it needs spectral preprocessing and calibration of image data [13]. Figure 4 show that SG smoothing has reduced the spectral noises significantly.

As shown in Figure 4, the hyperspectral spectrum has the relative reflectance intensity in the y-axis and the wavelength range in the x-axis. The x axis is associated with the wavelength ranges of the camera detector, lens, spectrograph, and halogen lamps of 400–1000 nm region. The visible-infrared spectrum has higher intensities in the region of 700–900 nm, the same fashion found in similar research of hyperspectral and infrared imaging on oil palm fresh fruit bunches [25], [27]. The measurement using four-band optical sensors showed higher reflectance intensities in the infrared region (700–900 nm) due to fewer absorbances by chlorophyll and anthocyanin in the mesocarp layer [22].
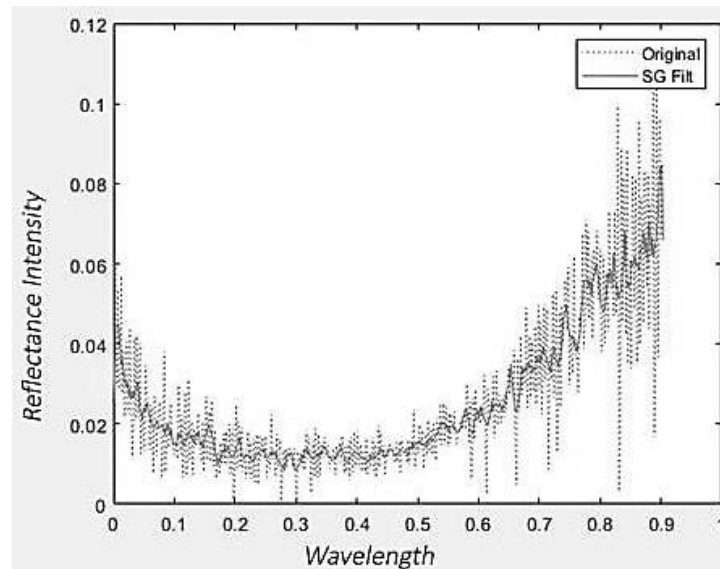
Figure 4. Original hyperspectral spectrum and after SG filtered

3.2. Displaying ANN results

The graphical user interface-GUI has been created for this study, which could be used for any hyperspectral data of oil palm FFBs. It had two buttons, which functioned to input hyperspectral images and to process and predict the result using the ANN. Figure 5 shows the GUI front view. In Figure 5, the front view of the GUI has two boxes for a hyperspectral image, the resulted spectra (left) and SG-filtered spectra (right).
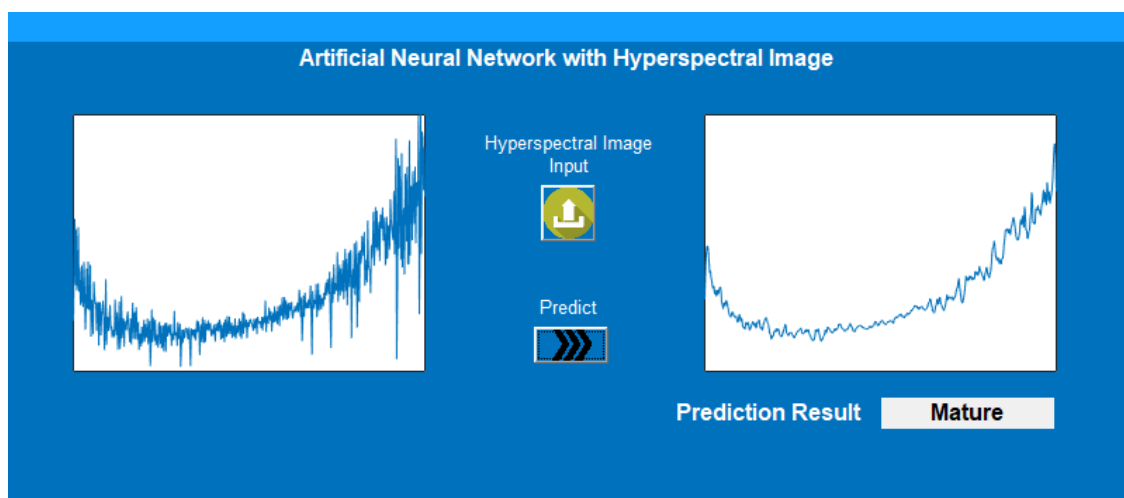

Figure 5. The GUI front view with spectral data input and the prediction result

The operation of the GUI starts by using the two available buttons. Each hyperspectral image is inserted automatically by clicking the <input hyperspectral image> button. The left box of the GUI shows the hyperspectral spectra of the inserted image. The next step is to process the hyperspectral data point. By clicking the button <predict>, the hyperspectral spectra are filtered by the SG filter algorithm and displayed on the right. The bottom right section shows the prediction result of ANN for oil palm FFB. The results have two options, immature (unripe) or mature (ripe). Oil palm FFBs arrived at the reception area of an oil palm mill are often categorized using two ripeness levels, unripe and ripe. Then the immature FFBs are separated. Other FFB conditions are related to external damages, such as rotten, empty, and long stalk FFBs. These categories need other sorting methods, such as object detection.

3.3. Testing data and prediction result

Results of testing the hyperspectral data of oil palm FFB using the k-fold cross-validation method had the highest accuracy for the 2nd fold, 5th fold, and 7th fold with 90 % accuracy. The results show that the n-fold cross validation method can measure the ANN accuracy. One of the standard metrics used to measure the performance of an ANN classifier based on k-fold validation is a mean squared error (MSE). Figure 6 shows the predicted and the actual result by the ANN model for the 7th fold prediction, which gives an MSE of 8.9924e-23. K-fold cross-validation works by finding the lowest MSE as the 'optimal' model. The discrepancy between the target and the ANN model could be due to the averaging effect [17] and noisy hyperspectral images.
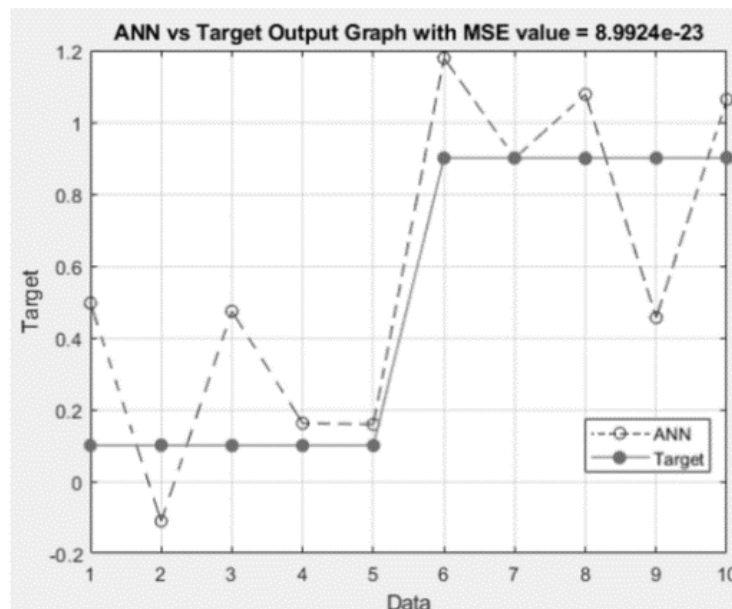

Figure 6. Comparison graph of prediction results and test data on 7-fold

3.4. Accuracy

Testing the ANN model using the k-fold cross validation method showed that each fold had a different accuracy. Table 3 shows the accuracy results of each fold for the ANN model in predicting the ripeness level of oil palm FFB. The accuracy calculation used positive and negative values represented by 1 and 0. The prediction results also used two states which are immature and mature. The immature state has a negative value, and the mature state has a positive value.

Table 3 shows the highest accuracies given by the 2nd fold, 5th fold, and 7th fold with 90% accuracy. The lowest accuracy was obtained by the 4th fold, followed by the 6th and 3rd fold, with accuracies below 75%. Lower accuracy on the 3rd fold, 4th fold, and 6th fold could be due to less k used. The k-fold cross-validation with more folds and a small number of replications should be used for performance evaluation [18].

Table 4 shows the evaluation of the ANN model used to predict the ripeness levels of oil palm FFB. Table 4 shows that the average accuracy for all seven folds is 79.17%. The result also displays that the highest accuracy belongs to the 2nd fold, 5th fold, and 7th fold. The results imply that the ANN model has a prediction category as <fair classification>. It also shows that the best dataset used for training the ANN

model is the dataset of the 7th fold, which gives an accuracy of 90% and is categorized as <excellent classification>. This result is slightly less by 5 % using similar hyperspectral imaging and ANN experiment of oil palm FFBs [27]. It was possibly due to the push broom scheme of hyperspectral imaging used in this study, where slightly unmatched the conveyor speed and frame rate per second (fps), creating blur images.

Table 3. Comparison of prediction results and testing data

Fold-n	Test data		Prediction result		Accuracy (%)
	Mature	Immature	Mature	Immature	
Fold-1	5	5	3	7	80
Fold-2	5	5	6	4	90
Fold-3	6	5	5	6	72.72
Fold-4	5	6	3	8	63.63
Fold-5	5	5	4	6	90
Fold-6	5	5	6	4	70
Fold-7	5	5	4	6	90

Table 4. Evaluation results of confusion matrix

Evaluation	Fold 1 (%)	Fold 2 (%)	Fold 3 (%)	Fold 4 (%)	Fold 5 (%)	Fold 6 (%)	Fold 7 (%)	Total (%)
Accuracy	80	90	72.72	63.63	90	70	90	79.17
Misclassification	20	10	27.27	36.36	10	30	10	20.83
Recall	37.5	55.56	50	28.57	44.44	57.14	44.44	45.61
Precision	100	83.33	80	66.67	100	66.67	100	83.87

4. CONCLUSION

This study aimed to investigate the potential use of an ANN and k-fold cross-validation to predict the ripeness levels of oil FFB. The prediction used hyperspectral images obtained using hyperspectral imaging. The ripeness levels were immature (unripe) and mature (ripe). SG filter was applied to smooth the hyperspectral data before being inserted into the neural network algorithm. The constructed ANN model used the k-fold cross-validation method to test its performance, which consisted of 7 folds. The evaluation performances of the testing used confusion matrix. The resulting confusion matrix parameters show that the average accuracy of the ANN model reaches 79.48%. The highest accuracies of 90 % belong to the 2nd fold, 5th fold, and 7th fold. The results showed that hyperspectral imaging with the SG filter, k-fold cross-validation, and ANN model is prospective to predict the ripeness levels of the oil palm FFB. These results will be the foundation toward using multispectral imaging in a rapid sorting and grading machine vision of oil palm FFBs.

REFERENCES

[1] M. F. A. Shaib, R. A. Rahim, S. Z. M. Muji, and A. A. A. Ahmad, "Investigating Maturity State and Internal Properties of Fruits Using Non-destructive Techniques-a Review," *TELKOMNIKA (Telecommunication Computing Electronics and Control)*, vol. 15, no. 4, pp. 1574–1584, Dec. 2017, doi: 10.12928/telkomnika.v15i4.7236.

[2] L. Kaiyan, L. Chang, S. Huiping, W. Junhui, and C. Jie, "Review on the Application of Machine Vision Algorithms in Fruit Grading Systems,"in *Advances in Intelligent Systems and Computing*, Dec 2021, vol. 1304, doi: 10.1007/978-3-030-63784-2_34.

[3] A. Bhargava and A. Bansal, "Fruits and vegetables quality evaluation using computer vision: A review," *Journal of King Saud University - Computer and Information Sciences*, vol. 33, no. 3, pp. 243–257, Mar. 2021, doi: 10.1016/j.jksuci.2018.06.002.

[4] F. He *et al.*, "Research progress in hyperspectral imaging technology for fruit quality detection," *Journal of Fruit Science*, vol. 38, no. 9, pp. 1590–1599, doi: 10.13925/j.cnki.gsxb.20210072.

[5] A. Hussain, H. Pu, and D.-W. Sun, "Innovative nondestructive imaging techniques for ripening and maturity of fruits – A review of recent applications," *Trends in Food Science & Technology*, vol. 72, pp. 144–152, Feb. 2018, doi: 10.1016/j.tifs.2017.12.010.

[6] H. Pu, Q. Wei, and D.-W. Sun, "Recent advances in muscle food safety evaluation: Hyperspectral imaging analyses and applications," *Critical Reviews in Food Science and Nutrition*, vol. 63, no. 10, pp. 1297–1313, Apr. 2023, doi: 10.1080/10408398.2022.2121805.

[7] X. Chen, T. Pang, H. Tao, M. Lin, and H. Yang, "Prediction of apple internal qualities using hyperspectral imaging techniques," in *2017 International Conference on Advanced Mechatronic Systems (ICAMechS)*, Dec. 2017, pp. 450–455, doi: 10.1109/ICAMechS.2017.8316516.

[8] A. Ibrahim *et al.*, "Preliminary Study for Inspecting Moisture Content, Dry Matter Content, and Firmness Parameters of Two Date Cultivars Using an NIR Hyperspectral Imaging System," *Frontiers in Bioengineering and Biotechnology*, vol. 9, Oct. 2021, doi: 10.3389/fbioe.2021.720630.

[9] J. J. V. Díaz, A. P. S. Aldana, and D. V. R. Zuluaga, "Prediction of dry matter content of recently harvested 'Hass' avocado fruits using hyperspectral imaging," *Journal of the Science of Food and Agriculture*, vol. 101, no. 3, pp. 897–906, Feb. 2021, doi: 10.1002/jsfa.10697.

[10] K. Hameed, D. Chai, and A. Rassau, "A comprehensive review of fruit and vegetable classification techniques," *Image and Vision Computing*, vol. 80, pp. 24–44, Dec. 2018, doi: 10.1016/j.imavis.2018.09.016.

[11] X. Yu, H. Lu, and D. Wu, "Development of deep learning method for predicting firmness and soluble solid content of postharvest Korla fragrant pear using Vis/NIR hyperspectral reflectance imaging," *Postharvest Biology and Technology*, vol. 141, pp. 39–49, Jul. 2018, doi: 10.1016/j.postharvbio.2018.02.013.

[12] Y. Xiang *et al.*, "Deep Learning and Hyperspectral Images Based Tomato Soluble Solids Content and Firmness Estimation," *Frontiers in Plant Science*, vol. 13, May 2022, doi: 10.3389/fpls.2022.860656.

[13] B. Jia *et al.*, "Essential processing methods of hyperspectral images of agricultural and food products," *Chemometrics and Intelligent Laboratory Systems*, vol. 198, Mar. 2020, doi: 10.1016/j.chemolab.2020.103936.

[14] J. Luo, K. Ying, and J. Bai, "Savitzky–Golay smoothing and differentiation filter for even number data," *Signal Processing*, vol. 85, no. 7, pp. 1429–1434, Jul. 2005, doi: 10.1016/j.sigpro.2005.02.002.

[15] Z. Zou *et al.*, "Detection of peanut seed vigor based on hyperspectral imaging and chemometrics," *Frontiers in Plant Science*, vol. 14, Feb. 2023, doi: 10.3389/fpls.2023.1127108.

[16] R. Raj, A. Cosgun, and D. Kulić, "Strawberry Water Content Estimation and Ripeness Classification Using Hyperspectral Sensing," *Agronomy*, vol. 12, no. 2, p. 425, Feb. 2022, doi: 10.3390/agronomy12020425.

[17] Y. Jung and J. Hu, "A K -fold averaging cross-validation procedure," *Journal of Nonparametric Statistics*, vol. 27, no. 2, pp. 167–179, Apr. 2015, doi: 10.1080/10485252.2015.1010532.

[18] T.-T. Wong and P.-Y. Yeh, "Reliable Accuracy Estimates from k -Fold Cross Validation," *IEEE Transactions on Knowledge and Data Engineering*, vol. 32, no. 8, pp. 1586–1594, Aug. 2020, doi: 10.1109/TKDE.2019.2912815.

[19] L. Aguni, S. Chabaa, S. Ibnyaich, and A. Zeroual, "Predicting the notch band frequency of an ultra-wideband antenna using artificial neural networks," *TELKOMNIKA (Telecommunication Computing Electronics and Control)*, vol. 19, no. 1, pp. 1–8, Feb. 2021, doi: 10.12928/telkomnika.v19i1.15912.

[20] V. Aredo, L. Velásquez, J. Carranza-Cabrera, and R. Siche, "Predicting of the Quality Attributes of Orange Fruit Using Hyperspec-tral Images," *Journal of Food Quality and Hazards Control*, vol. 6, no. 3, pp. 82–92, Aug. 2019, doi: 10.18502/jfqhc.6.3.1381.

[21] C. M. Abazue, E. A. Choy, and N. Lydon, "Oil palm smallholders and certification: exploring the knowledge level of independent oil palm smallholders to certification," *Journal of Bioscience and Agriculture Research*, vol. 19, no. 1, pp. 1589–1596, 2019, doi: 10.18801/jbar.190119.193.

[22] S. L. Utom *et al.*, "Non-Destructive Oil Palm Fresh Fruit Bunch (FFB) Grading Technique Using Optical Sensor," *International Journal of Integrated Engineering*, vol. 10, no. 1, pp. 35–39, Apr. 2018, doi: 10.30880/ijie.2018.10.01.006.

[23] S. Zolfagharnassab, A. R. B. M. Shariff, R. Ehsani, H. Z. Jaafar, and I. Bin Aris, "Classification of Oil Palm Fresh Fruit Bunches Based on Their Maturity Using Thermal Imaging Technique," *Agriculture*, vol. 12, no. 11, pp. 1–20, Oct. 2022, doi: 10.3390/agriculture12111779.

[24] H. Ishak, M. Shiddiq, R. H. Fitra, and N. Z. Yasmin, "Ripeness Level Classification of Oil Palm Fresh Fruit Bunch Using Laser Induced Fluorescence Imaging," *Journal of Aceh Physics Society*, vol. 8, no. 3, pp. 84–89, Sep. 2019, doi: 10.24815/jacps.v8i3.14139.

[25] Z. Iqbal, S. Herodian, and S. Widodo, "Development of Partial Least Square (PLS) Prediction Model to Measure the Ripeness of Oil Palm Fresh Fruit Bunch (FFB) by Using NIR Spectroscopy," *IOP Conference Series: Earth and Environmental Science*, vol. 347, no. 1, p. 012079, Nov. 2019, doi: 10.1088/1755-1315/347/1/012079.

[26] F. Candra and S. A. R. A. Bakar, "Hyperspectral Imaging for Predicting Soluble Solid Content of Starfruit," *Jurnal Teknologi*, vol. 73, no. 1, Feb. 2015, doi: 10.11113/jt.v73.3480.

[27] O. M. Bensaeed, A. M. Shariff, A. B. Mahmud, H. Shafri, and M. Alfatni, "Oil palm fruit grading using a hyperspectral device and machine learning algorithm," *IOP Conference Series: Earth and Environmental Science*, vol. 20, pp. 1–22, Jun. 2014, doi: 10.1088/1755-1315/20/1/012017.

[28] H. Jiang, Y. Hu, X. Jiang, and H. Zhou, "Maturity Stage Discrimination of Camellia oleifera Fruit Using Visible and Near-Infrared Hyperspectral Imaging," *Molecules*, vol. 27, no. 19, pp. 1–14, Sep. 2022, doi: 10.3390/molecules27196318.

[29] S. Naaz, "Detection of Phishing in Internet of Things Using Machine Learning Approach," *International Journal of Digital Crime and Forensics*, vol. 13, no. 2, pp. 1–15, Mar. 2021, doi: 10.4018/IJDCF.2021030101.

[30] P. Koziol *et al.*, "Comparison of spectral and spatial denoising techniques in the context of High Definition FT-IR imaging hyperspectral data," *Scientific Reports*, vol. 8, no. 1, pp. 1–11, Sep. 2018, doi: 10.1038/s41598-018-32713-7.

BIOGRAPHIES OF AUTHORS

Minarni Shiddiq 🆔 🔍 SC ◗ is a full professor at Department of Physics, Faculty of Mathematics and Science, Universitas Riau. Her current research interests include optoelectronic systems, hyperspectral and multispectral imaging, computer vision, and machine vision, and laser applications. She is currently working in implementing hyperspectral and multispectral imaging in sorting and grading oil palm fresh fruits and plastics sortation. She can be contacted at email: minarni.shidddiq@lecturer.unri.ac.id.

Feri Candra (iD) (g) SC ⟳ is an associate professor at the Department of Electrical Engineering, Faculty of Engineering, Universitas Riau. His current research interests include hyperspectral imaging, machine learning, embedded systems, robotics, and computer vision. He is currently working in a robotic for helping COVID patients. He can be contacted at email: feri@eng.unri.ac.id.

Barri Anand (iD) (g) SC ⟳ was a student at Universitas Riau in 2016 and has finished studying Information Engineering at Department of Electrical Engineering, Universitas Riau with a B.Eng. degree in 2019. His research interests include machine learning and imaging. He can be contacted at email: barryanand95@gmail.com.

Mohammad Fisal Rabin (iD) (g) SC ⟳ was a student at Universitas Riau 2014 and has finished studying Physics at Department of Physics, Universitas Riau with a B.Sc. degree in 2019. His research interests include hyperspectral imaging and automation. He has just graduated for his M.Sc. from the same Department of Physics and working in building a LED based multispectral imaging for oil palm FFB ripeness detection. He can be contacted at email: fisal.rabin25@gmail.com.